Supported Catalysts

Deutsche Ausgabe: DOI: 10.1002/ange.201505867
Internationale Ausgabe: DOI: 10.1002/anie.201505867

Iridium(I)/N-Heterocyclic Carbene Hybrid Materials: Surface Stabilization of Low-Valent Iridium Species for High Catalytic Hydrogenation Performance

Iuliia Romanenko, David Gajan, Reine Sayah, Delphine Crozet, Erwan Jeanneau, Christine Lucas, Lénaic Leroux, Laurent Veyre, Anne Lesage, Lyndon Emsley, Emmanuel Lacôte, and Chloé Thieuleux**

Abstract: *An Ir^{I}(NHC)-based hybrid material was prepared using a methodology which allowed the precise positioning and isolation of the Ir centers along the pore channels of a silica framework. The full characterization of the material by solid-state NMR spectroscopy showed that the supported Ir sites were stabilized by the silica surface, as low-coordinated single-site complexes. The material is extremely efficient for the hydrogenation of functional alkenes. The catalytic performance (TOF and TON) is one to two orders of magnitude higher than those of their molecular Ir analogues, and could be related to the prevention of the bimolecular deactivation of Ir complexes observed under homogeneous conditions.*

Catalytic hydrogenation is one of the most important reactions for both bulk and fine-chemical production.[1] As a consequence, the quest for evermore active and selective catalytic systems is essential. Late transition metal complexes stand out among the numerous options because their coordination sphere can be fine-tuned for better efficiency, selectivity, and stereoselectivity. This is especially true for iridium, one of the most active metals for catalytic hydrogenation.[2] However, in solution, iridium complexes tend to rapidly form inactive polymetallic hydride clusters through bimolecular processes, thus leading to deactivation.[3]

One strategy to prevent this deactivation path is to slow down the oligomerization of the iridium hydrides in solution by modifying the coordination sphere of the iridium[4a] or using weakly coordinating anions (for cationic Ir^{I} catalysts).[4b,c] Another option is to graft or intercalate the iridium(I) sites on a solid support, to physically prevent them from assembling into inactive clusters.[5] The latter is appealing because heterogeneous catalysts are easier to remove from products. However, the "heterogeneized" catalysts prepared by grafting or intercalation approaches usually exhibit low to similar activity in comparison with their homogeneous equivalents.[5a–d] We hypothesized that this decrease of activity was due to a lack of control of the metal distribution on the solid supports, and that hybrid materials containing strongly coordinated and precisely positioned supported iridium(I) sites would be much more efficient hydrogenation catalysts.

In this respect, we proposed a general strategy for the preparation of late transition metal-based catalytic materials, a strategy which relies on a two-step approach.[6] The first step is the preparation of hybrid mesostructured silica matrices containing regularly distributed L-type ligands by a sol-gel process using a templating route.[7] The L-ligand of the platform material is then converted in situ into the targeted supported organometallic complex by surface organometallic chemistry (SOMC).[8]

The hybrid silica material is prepared by co-hydrolysis and co-condensation of an organo-trialkoxysilane precursor and a tetra-alkoxysilane in the presence of a structure-directing agent to control the loading and homogeneity of the organic groups along the silica pore channels. This control is mandatory to ensure that the catalytically active sites in the final material are appropriately isolated from each other. By using this methodology, we have investigated the immobilization on silica matrices of reactive Pd^{II},[6c] Ru^{IV},[6d,e] and Ir^{III}[6b] species, as their N-heterocyclic carbene (NHC) complexes. The resulting materials are as active as their molecular equivalents.

Here, we coordinate iridium(I) centers to a silica-supported NHC ligand, because the Ir–NHC bond is strong[9] and NHCs also offer a good alternative to the phosphine ligands classically used in iridium-catalyzed hydrogenation.[2a] A flexible propyl tether was chosen to allow Ir–silica interactions. Such a metal–support interaction was found to be the key for increasing the lifetime of Ru(NHC) active species by stabilizing low-valent species,[6e] and we felt that it might be extended to stripped-down Ir(NHC) complexes, thus leading to even more active catalysts (see **M-Ir** in Scheme 1).

The preparation of the materials relies on the incorporation of iridium onto our previously described NHC-based

---

[*] I. Romanenko, Dr. R. Sayah, Dr. D. Crozet, C. Lucas, L. Veyre, Dr. E. Lacôte, Dr. C. Thieuleux
Université de Lyon, Institut de Chimie de Lyon, UMR C2P2 CNRS, Université Lyon 1-ESCPE Lyon
43 Bd du 11 Novembre 1918, 69616 Villeurbanne (France)
E-mail: emmanuel.lacote@univ-lyon1.fr
chloe.thieuleux@univ-lyon1.fr

Dr. D. Gajan, L. Leroux, Dr. A. Lesage, Prof. L. Emsley
Université de Lyon, Institut des Sciences Analytiques
CRMN CNRS-ENS Lyon-UCBL, 69100 Villeurbanne (France)

Dr. E. Jeanneau
Université Lyon 1, Centre de Diffractométrie H. Longchambon
Site CLEA—Bât. ISA, 69100 Villeurbanne (France)

Prof. L. Emsley
Institut des Sciences et Ingénierie Chimiques, Ecole Polytechnique Fédérale de Lausanne (EPFL), 1015 Lausanne (Switzerland)

Supporting information for this article is available on the WWW under http://dx.doi.org/10.1002/anie.201505867.

© 2015 Wiley-VCH Verlag GmbH & Co. KGaA, Weinheim

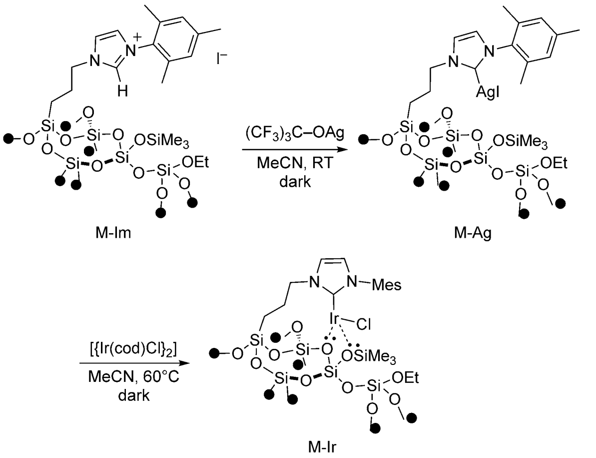

Scheme 1. Scheme for the preparation of the hybrid catalyst **M-Ir**.

material **M-Im** (Scheme 1).[6b] The passivated platform material **M-Im** (390 $m^2 g^{-1}$ surface area) was first metalated to the silver-carbene-containing material **M-Ag** with 1.5 equivalents of $AgOC(CF_3)_3$ in MeCN at 25 °C in the absence of light. Transmetalation with 7 equivalents of $[\{IrCl(cod)\}_2]$ (cod = 1,5-cyclooctadiene) at 60 °C in MeCN delivered **M-Ir** as a brown powder containing 2.57 wt% Ir (0.13 $mmol g^{-1}$), thus corresponding to a 49% silver to iridium conversion. **M-Ir** was characterized by XRD (see Figure S1 in the Supporting Information), TEM (see Figure S2), and conventional ^{13}C, ^{29}Si MAS-NMR spectroscopy (see Figures S3 and S4), as well as DNP SENS. We also prepared the ^{13}C-labeled material **M*-Ir** from the corresponding **M*-Im**, wherein the carbene carbon atom was isotopically enriched. Finally, the complex [IrCl(cod)(MesImPr)] (**1**) was synthesized by a known route[10] and characterized by HRMS, as well as ^1H, ^{13}C, and ^1H-^{13}C HMQC NMR spectroscopy (see Figure S5). The XRD structure of **1** was also elucidated (see Figure S6).[11] This complex was prepared as a molecular standard for both materials characterization and for the sake of comparison in the catalytic study.

The most important feature in **1** is that the iridium complex loses symmetry upon transmetalation because of its square-planar structure and the dissymmetry of the NHC ligand. Thus, all carbon atoms of the cod ligand are inequivalent. The methylene ^{13}C signals in C_6D_6 appear at $\delta = 29.4$, 29.1, 33.3, and 34.9 ppm, while the sp^2 carbon atoms are at $\delta = 50.3$, 51.1 (*trans* to Cl), and 83.1 and 83.2 ppm (*trans* to NHC).

The ^{29}Si CPMAS NMR spectra of **M-Ir** shows the presence of the four expected peaks: $\delta = 13$ (M), −65 (T_3), −100 (Q_3), −109 ppm (Q_4; see Figure S3). The first peak corresponds to the $SiMe_3$ surface groups and shows that passivation was successful, while the presence of a T_3 peak shows that the organosilane residue is completely fused within the silica network, thus leading to a fully condensed tetrahedral Si surface site. In the ^{13}C CPMAS NMR spectrum (see Figure S4), the expected signals arising from the propyl tether and the NHC ligand were observed around $\delta = 9$ ppm ($Si\text{-}CH_2$), $\delta = 18\text{-}20$ ppm (methyl groups of the mesityl substituent and $Si\text{-}CH_2\text{-}CH_2$), $\delta = 52$ ppm (CH_2-N), and $\delta = 120$–140 ppm (aryl and NHC sp^2 carbons). Interestingly, the ^{13}C peaks corresponding to the cod ligand were not detected.

TEM micrographs and EDX analyses showed the presence of silver aggregates arising from production of the silver halide salt during the transmetalation process. TEM micrographs do not indicate the presence of any iridium nanoparticles, and EDX, performed on several zones of the material, provided similar iridium loadings, thus suggesting a homogeneous distribution of the iridium throughout all the material (see Figure S7). These observations suggest that iridium is present as a supported coordination complex, not as metal nanoparticles.

To shed light on the nature of the iridium species, and their possible interaction with the silica surface, we compared the two-dimensional (2D) HETCOR NMR spectra of the labeled materials **M*-Im**, **M*-Ag**, and **M*-Ir** at long (Figure 1; see Figure S10) and short (see Figure S11) contact times to discriminate directly bonded ^1H and ^{13}C versus spatially close ^1H and ^{13}C atoms. At a long contact time, correlation spots were found between the protons of the surface trimethylsilyl (TMS) groups and the aromatic carbon atoms of the mesityl for all materials, thus suggesting that the NHC is folded toward the surface. More interestingly, the sole crosspeak assigned to the carbene in the ^1H-^{13}C HETCOR of **M*-Ag**

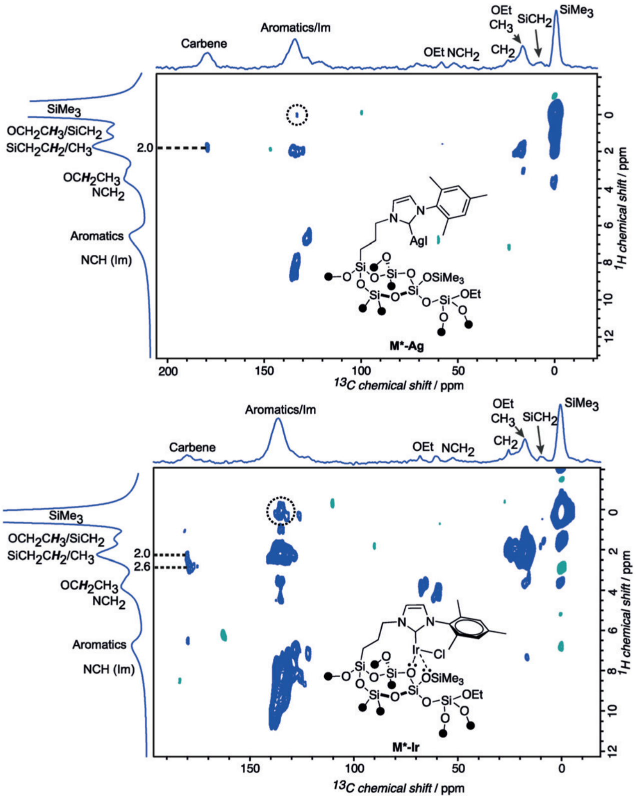

Figure 1. 2D ^1H-^{13}C HETCOR NMR spectra of **M*-Ag** and **M*-Ir** recorded on a 800 MHz with a long contact time (2 ms). Traces along the top are the corresponding one-dimensional (1D) ^{13}C CPMAS spectra and the traces along the left are the corresponding 1D ^1H Hahn echo spectra. (see the Supporting Information for experimental details).

© 2015 Wiley-VCH Verlag GmbH & Co. KGaA, Weinheim

(Figure 1, top) is split after iridium transmetallation (Figure 1, bottom). This split is attributed to the formation of the Ir(NHC) along with residual Ag(NHC) species. This observation is consistent with a splitting of the NMR signal of the same methyl groups in **1**. Here again, no signal attributed to cod was detected, thus strongly suggesting its absence in the iridium coordination sphere. Taking into account that the NHC folds toward the surface, one may hypothesize that the iridium sites are stabilized by surface Si-O-Si groups after decoordination of 1,5-cyclooctadiene. To discard any possible uncertainty resulting from the limited sensitivity of conventional MAS NMR, we implemented advanced dynamic nuclear polarization surface enhanced NMR spectroscopy (DNP SENS) experiments.[12] The samples were prepared by impregnation of the materials with a solution of 16 mM TEKPOL in 1,1,2,2-tetrachloroethane and the spectra were recorded on a 400 MHz/263 GHz gyrotron DNP NMR system. In this setup, EPR transitions of the radical are saturated at 100 K by microwaves, which induce transfer of the electron spin polarization to nuclei of interest at the silica surface, thus resulting in large NMR signal enhancement.

Again, no signal in the cod region was detected in the ^{13}C DNP SENS experiments (Figure 2; see Figure S12). Similarly, no correlation signal involving a cod was observed in 2D DNP SENS ^{1}H-^{13}C HETCOR spectra (see Figure S13). However, 2D DNP SENS ^{1}H-^{29}Si HETCOR spectra (see Figure S14a) showed a correlation between Q signals at $\delta = -100$ ppm and the NHC backbone, as well as mesityl protons, even with short contact times. At longer contact times (see Figure S14b), crosspeaks between the $SiMe_3$ and the aromatics also appeared. As this method assesses the spatial proximity of protons to the silicon centers,[12b] this data further suggests that the spacer folds toward the surface to stabilize a cod-free iridium species.

We finally attempted to prove the absence/presence of cod by a chemical method. We exposed a C_6D_6 suspension containing **M-Ir** and toluene, as an internal standard, to hydrogen in a pressure-stable NMR tube without an olefinic substrate, and monitored the reaction by solution ^{1}H NMR spectroscopy. We were able to detect trace amounts of cyclooctane, whose quantification against toluene (see Figures S15 and S16) revealed that only 8 % of iridium sites contain cod.[13]

To conclude, our NMR study combined with further chemical reactivity directly point to the presence of surface–metal interactions which stabilize a supported low-coordinated iridium complex (see Figure 1 for a tentative proposed structure). These novel spectroscopic and chemical data are in agreement with our previous proposals on a closely related ruthenium system,[6e] albeit the direct evidence was limited to 1D ^{31}P NMR spectrum at the time.

The catalytic activity of the **M-Ir** material was tested in the hydrogenation of several functional substrates, that is, styrenes with various substituents, stilbene, and limonene (see Table S4). In a typical catalytic experiment, a solution of *trans*-stilbene in toluene was heated at 40 °C in a Fisher–Porter reactor under 3 bar of dihydrogen in the presence of 0.1 mol % **M-Ir** (based on iridium loading given by elemental analysis). The reaction was monitored by solution NMR spectroscopy to observe a conversion versus time profile (Figure 3). Full conversion was observed after 18 h. The same reaction using **1** under homogeneous conditions failed to reach full conversion after more than 80 days. The cationic iridium species [Ir(cod)(MesImPr)]BF_4, generated in situ from [IrCl(cod)(MesImPr)] with $AgBF_4$ under homogeneous conditions, worked faster but even then the reaction was not over after 60 days. Moreover, a blank test using the parent material **M-Ag** left the substrate unchanged, thus showing that catalysis was due to the iridium centers in the material.

We calculated the initial turnover frequencies (TOFs; after 5 h of reaction) for **M-Ir**, the neutral complex **1**, and its cationic form: TOF = 38 h^{-1} for **M-Ir** versus 1.8 h^{-1} for [Ir(cod)(MesImPr)]BF_4, and 0.75 h^{-1} for **1**. The material is

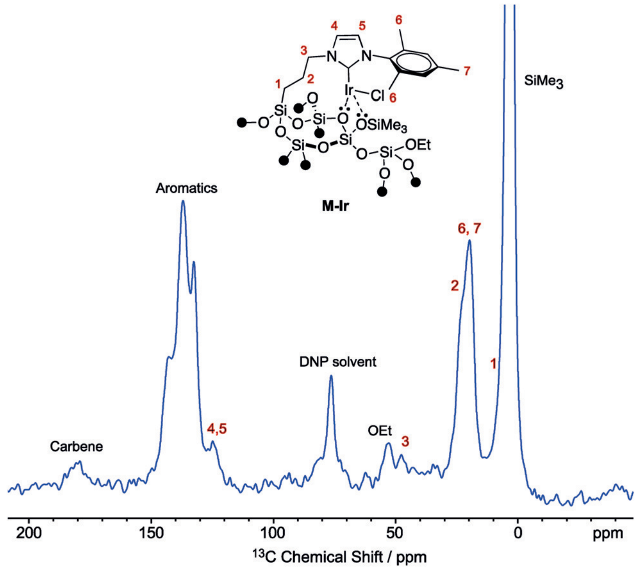

Figure 2. ^{13}C CP MAS solid echo DNP SENS spectrum of **M-Ir** recorded on a 400 MHz DNP NMR system with an echo time of 40 rotor periods (see the Supporting Information for details).

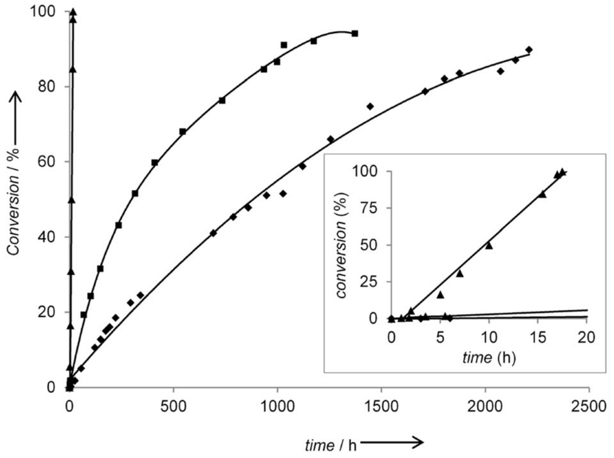

Figure 3. Conversion of *trans*-stilbene, under hydrogenation conditions, as a function of reaction time using: neutral organometallic complex **1** (◆); cationic [Ir(cod)(MesImPr)]BF_4 (■); **M-Ir** material (▲). The hydrogenation experiments were carried out in toluene at 40 °C under 3 bar of H_2 (0.1 mol % of Ir).

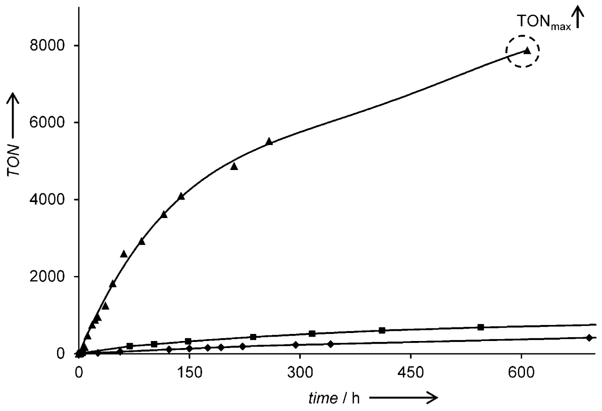

Figure 4. TON for the hydrogenation of *trans*-stilbene as a function of reaction time using: **1** (◆); [Ir(cod)(MesImPr)]BF_4 (■); **M-Ir** (▲). The hydrogenation experiments were carried out in toluene at 40 °C under 3 bar of H_2 (0.1 mol% of Ir for **1** and [Ir(cod)(MesImPr)]BF_4; 0.01 mol% of Ir for **M-Ir**).

thus 50 times faster than **1**, and 20 times faster than [Ir(cod)(MesImPr)]BF_4, thus fully validating our hypotheses. Furthermore, the hydrogenation profile of **M-Ir** in Figure 3 is linear and suggests that there is no catalyst deactivation during the catalytic test.

We evaluated the heterogeneous catalyst activity using very high substrate/catalyst ratios (0.01 mol%; Figure 4). While both homogeneous complexes are deactivated and only reach a $TON_{max} \leq 1000$ (turnover number) after 700 hours (observation of the catalyst deactivation at 89% conversion using 0.1 mol% of **1**), **M-Ir** exhibited a much higher productivity, thus reaching 80% conversion ($TON = 8000$ using 0.01 mol% of **M-Ir**). After catalysis, the solid was analyzed by HRTEM. We did not see any trace of Ir nanoparticles in the recovered catalyst. Unfortunately, we could not determine the TON_{max}. The trace impurities remaining after purification of the large amounts of solvent and substrate needed for the tests induced side poisoning of the 60 mg of catalyst needed for reproducibility at the high substrate/Ir ratios required for TON_{max} determination.

Split tests were carried out using **M-Ir** (see Figure S19). No conversion was detected, thus showing the absence of any active iridium species in solution. Finally, no leaching of iridium was detected by ICP measurements on the reaction supernatants. Therefore there is no contribution of any homogeneous pathway. The catalytic hydrogenation takes place on iridium surface sites of the material.

The behavior of other substrates (styrene, 4-fluorostyrene, 4-vinylanisole, 4-acetoxystyrene and limonene) is shown in the Supporting Information. In all cases, the material is better than **1** (see Figure S18 and part 7 of the Supporting Information). For limonene, the less hindered bond is fully hydrogenated before the more-substituted one started reacting.

In summary, we have prepared a well-defined single-site Ir^{I}(NHC)-based heterogeneous catalyst in which the iridium atoms are homogeneously positioned by design. By using advanced solid-state NMR techniques, and a chemical method we showed that the iridium centers are stabilized, by the surface, as low-coordinated complexes. This catalytic material is one to two orders of magnitude more active and faster than its molecular analogue in the hydrogenation of *trans*-stilbene, and also faster than the corresponding cationic species. This enhanced activity was also observed for other functional olefins. It derives from the isolation of the supported Ir(NHC) species, which prevents the bimolecular deactivation processes (hydride cluster formation) usually encountered for iridium complexes in solution. Interactions between the silica surface and the iridium sites, which stabilize a low-valent iridium(I) species, were evidenced for the first time. They likely also account for the higher catalytic performances of **M-Ir**.[14]

The strategy wherein more-active catalysts are obtained by preventing deactivation of bimolecular processes and by using a support to stabilize the more-reactive species is of interest for many other catalytic systems. Further work will focus on extending this approach towards the preparation of highly selective asymmetric heterogeneous iridium catalysts.

Acknowledgements

We thank CNRS, CPE, Université Claude Bernard Lyon 1, ANR (CFLOW-OM, NHCX), and Total (postdoctoral funding to D.C.) for financial support of this work. I.R. thanks CNRS/CPE for a doctoral stipend. TGIR RMN THC (FR 3050 CNRS) and ERC Advanced grant number 320860, are kindly acknowledged for the NMR characterizations. We thank the Centre Technologique des Microstructures (CTμ) for the TEM measurements.

Keywords: carbenes · hydrogenation · iridium · solid-state structures · supported catalysts

How to cite: *Angew. Chem. Int. Ed.* **2015**, *54*, 12937–12941
Angew. Chem. **2015**, *127*, 13129–13133

---

[1] a) *The Handbook of Hydrogenation* (Eds.: J. G. de Vries, C. J. Elsevier), Wiley-VCH, Weinheim, **2007**; b) W. S. Knowles, *Angew. Chem. Int. Ed.* **2002**, *41*, 1998–2007; *Angew. Chem.* **2002**, *114*, 2096–2107; c) W. Bonrath, J. Medlock, J. Schütz, B. Wüstenberg, T. Netscher in *Hydrogenation* (Eds.: I. Karame), InTech, Open Access, **2012**, pp. 69–90.

[2] a) *Iridium complexes in organic synthesis* (Eds.: L. Oro, C. Claver), Wiley-VCH, Weinheim, **2008**; b) *Iridium Catalysis, Topics in Organometallic Chemistry*, *Vol. 34* (Ed.: P. G. Andersson), Springer, Berlin, **2011**, pp. 1–76; c) R. Crabtree, *Acc. Chem. Res.* **1979**, *12*, 331–337.

[3] a) Y. Xu, M. A. Celik, A. L. Thompson, H. Cai, M. Yurtsever, B. Odell, J. C. Green, D. M. P. Mingos, J. M. Brown, *Angew. Chem. Int. Ed.* **2009**, *48*, 582–585; *Angew. Chem.* **2009**, *121*, 590–593; b) S. P. Smidt, A. Pfaltz, E. Martínez-Viviente, P. S. Pregosin, A. Albinati, *Organometallics* **2003**, *22*, 1000–1009; c) X. Cui, Y. Fan, M. B. Hall, K. Burgess, *Chem. Eur. J.* **2005**, *11*, 6859–6868; d) L. D. Vazquez-Serrano, B. T. Owens, J. M. Buriak, *Chem. Commun.* **2002**, 2518–2519; e) J. Campos, L. S. Sharninghausen, R. H. Crabtree, D. Balcells, *Angew. Chem. Int. Ed.* **2014**, *53*, 12808–12811; *Angew. Chem.* **2014**, *126*, 13022–13025; f) *Homogeneous Catalysts: Activity—Stability—Deactivation*, 1st ed. (Eds.: P. W. N. M. van Leeuwen, J. C. Chadwick), Wiley-VCH, Weinheim, **2011**.

© 2015 Wiley-VCH Verlag GmbH & Co. KGaA, Weinheim

[4] a) Y. Xu, D. M. P. Mingos, J. M. Brown, *Chem. Commun.* **2008**, 199 – 201; b) S. P. Smidt, N. Zimmermann, M. Studer, A. Pfaltz, *Chem. Eur. J.* **2004**, *10*, 4685 – 4693; c) S. Gruber, M. Neuburger, A. Pfaltz, *Organometallics* **2013**, *32*, 4702 – 4711; d) L. D. Vazquez-Serrano, B. T. Owens, J. M. Buriak, *Inorg. Chim. Acta* **2006**, *359*, 2786 – 2797.

[5] For Ir catalysts heterogeneized on silica supports, see: a) B. Pugin, H. Landert, F. Spindler, H.-U. Blaser, *Adv. Synth. Catal.* **2002**, *344*, 974 – 979; b) C. González-Arellano, A. Corma, M. Iglesias, F. Sánchez, *Inorg. Chim. Acta* **2004**, *357*, 3071 – 3078; c) S. Sahoo, P. Kumar, F. Lefebvre, S. B. Halligudi, *J. Catal.* **2008**, *254*, 91 – 100; for other types of supports d) M. Crocket, R. H. M. Herold, *Catal. Lett.* **1993**, *18*, 243 – 251; e) M. Blanco, P. Álvarez, C. Blanco, M. Vi. Jiménez, J. Fernández-Tornos, J. J. Pérez-Torrente, L. A. Oro, R. Menéndez, *ACS Catal.* **2013**, *3*, 1307 – 1317.

[6] a) M. P. Conley, C. Copéret, C. Thieuleux, *ACS Catal.* **2014**, *4*, 1458 – 1469; b) T. K. Maishal, J. Alauzun, J.-M. Basset, C. Copéret, R. J. P. Corriu, E. Jeanneau, A. Mehdi, C. Reyé, L. Veyre, C. Thieuleux, *Angew. Chem. Int. Ed.* **2008**, *47*, 8654 – 8656; *Angew. Chem.* **2008**, *120*, 8782 – 8784; c) M. P. Conley, R. M. Drost, M. Baffert, D. Gajan, C. Elsevier, W. T. Franks, H. Oschkinat, L. Veyre, A. Zagdoun, A. Rossini, M. Lelli, A. Lesage, G. Casano, O. Ouari, P. Tordo, L. Emsley, C. Copéret, C. Thieuleux, *Chem. Eur. J.* **2013**, *19*, 12234 – 12238; d) I. Karamé, M. Boualleg, J.-M. Camus, T. K. Maishal, J. Alauzun, J.-M. Basset, C. Copéret, R. J. P. Corriu, E. Jeanneau, A. Mehdi, C. Reyé, L. Veyre, C. Thieuleux, *Chem. Eur. J.* **2009**, *15*, 11820 – 11823; e) M. K. Samantaray, J. Alauzun, D. Gajan, S. Kavitake, A. Mehdi, L. Veyre, M. Lelli, A. Lesage, L. Emsley, C. Copéret, C. Thieuleux, *J. Am. Chem. Soc.* **2013**, *135*, 3193 – 3199.

[7] a) S. L. Burkett, S. D. Sims, S. Mann, *Chem. Commun.* **1996**, 1367 – 1368; b) D. J. Macquarrie, *Chem. Commun.* **1996**, 1961 – 1962; c) D. Margolese, J. A. Melero, S. C. Christiansen, B. F. Chmelka, G. D. Stucky, *Chem. Mater.* **2000**, *12*, 2448 – 2459; d) L. Mercier, T. J. Pinnavaia, *Chem. Mater.* **2000**, *12*, 188 – 196; For a review, see: e) F. Hoffmann, M. Cornelius, J. Morell, M. Fröba, *Angew. Chem. Int. Ed.* **2006**, *45*, 3216 – 3251; *Angew. Chem.* **2006**, *118*, 3290 – 3328.

[8] C. Copéret, M. Chabanas, R. Petroff Saint-Arroman, J.-M. Basset, *Angew. Chem. Int. Ed.* **2003**, *42*, 156 – 181; *Angew. Chem.* **2003**, *115*, 164 – 191.

[9] a) H. M. Lee, T. Jiang, E. D. Stevens, S. P. Nolan, *Organometallics* **2001**, *20*, 1255 – 1258; b) M. T. Powell, D.-R. Hou, M. C. Perry, X. Cui, K. Burgess, *J. Am. Chem. Soc.* **2001**, *123*, 8878 – 8879; c) Y. Zhu, Y. Fan, K. Burgess, *J. Am. Chem. Soc.* **2010**, *132*, 6249 – 6253; d) I. Kownacki, M. Kubicki, K. Szubert, B. Marciniec, *J. Organomet. Chem.* **2008**, *693*, 321 – 328; e) G. E. Dobereiner, A. Nova, N. D. Schley, N. Hazari, S. J. Miller, O. Eisenstein, R. H. Crabtree, *J. Am. Chem. Soc.* **2011**, *133*, 7547 – 7562; f) L. S. Bennie, C. J. Fraser, S. Irvine, W. J. Kerr, S. Andersson, G. Nilsson, *Chem. Commun.* **2011**, *47*, 11653 – 11655; g) *N-Heterocyclic Carbenes: Effective Tools for Organometallic Synthesis*, 1st ed. (Ed.: S. P. Nolan), Wiley-VCH, Weinheim, **2014**.

[10] H. M. J. Wang, I. J. B. Lin, *Organometallics* **1998**, *17*, 972 – 975.

[11] CCDC 1043116 contains the supplementary crystallographic data for this paper. These data can be obtained free of charge from The Cambridge Crystallographic Data Centre.

[12] a) A. Lesage, M. Lelli, D. Gajan, M. A. Caporini, V. Vitzthum, P. Miéville, J. Alauzun, A. Roussey, C. Thieuleux, A. Mehdi, G. Bodenhausen, C. Copéret, L. Emsley, *J. Am. Chem. Soc.* **2010**, *132*, 15459 – 15461; b) M. Lelli, D. Gajan, A. Lesage, M. A. Caporini, V. Vitzthum, P. Mieville, F. Heroguel, F. Rascon, A. Roussey, C. Thieuleux, M. Boualleg, L. Veyre, G. Bodenhausen, C. Coperet, L. Emsley, *J. Am. Chem. Soc.* **2011**, *133*, 2104 – 2107; For a review, see: c) A. Rossini, A. Zagdoun, M. Lelli, A. Lesage, C. Copéret, L. Emsley, *Acc. Chem. Res.* **2013**, *46*, 1942 – 1951.

[13] Besides the evolution of cod, the hydrogenation of C_6D_6 was observed, as shown by the growth of a broad signal at ca. $\delta =$ 1.37 ppm, which corresponds to deuterated cyclohexane. This result and the slight color modification suggest the formation of iridium nanoparticles in that case. For a reference on the room-temperature hydrogenation of benzene with iridium nanoparticles, see: E. Bayram, M. Zahmakiran, S. Özkar, R. G. Finke, *Langmuir* **2010**, *26*, 12455 – 12464. The presence of iridium nanoparticles in the spent catalysts was further confirmed by TEM and EDX analyses (see Figure S17).

[14] M. Rimoldi, A. Mezzetti, *Inorg. Chem.* **2014**, *53*, 11974 – 11984.

Received: June 26, 2015
Revised: July 24, 2015
Published online: September 4, 2015

© 2015 Wiley-VCH Verlag GmbH & Co. KGaA, Weinheim